Effect of post-earthquake rainfall in triggering landslides

Effet des précipitations après le séisme dans le déclenchement des glissements de terrain

Binod Tiwari, Beena Ajmera, Duc Tran, Santiago Caballero
Civil and Environmental Engineering Department, California State University, Fullerton, USA, btiwari@fullerton.edu

ABSTRACT: In this study, a systematic evaluation of the effect of void ratio, intensity and duration of rainfall, and slope inclination on seepage velocity and stability for static slopes as well as slopes subjected post-earthquake rainfall events was performed. Soil samples were collected from a slope failure site in a residential area in Southern California and compacted in a Plexiglas container at three different void ratios and three different inclinations. Those slopes were instrumented with several miniature tensiometers and displacement measurement devices at different depths and then, subjected to two different intensities of rainfall until the entire slope became saturated. Variation in suction and advancement of wetting front were recorded at a regular interval to calculate the seepage velocity. Moreover, a slope, instrumented with numerous accelerometers, was first shaken on a shake table with various amplitudes and frequencies of seismic motions and then, subjected to a rainfall event to evaluate the change in suction and seepage velocity after the shaking events. The experimental results, verified by numerical analyses were used to evaluate the relationship between rainfall intensity, void ratio, slope inclination, and the corresponding stability of the slope.

Résumé: Dans cette étude, une évaluation systématique de l'effet du taux de vide, de l'intensité et de la durée des précipitations et de l'inclinaison de la pente sur la vitesse d'infiltration et la stabilité des pentes statiques ainsi que des pentes soumises aux précipitations post-séismiques ont été effectuées. Des échantillons de sol ont été prélevés dans un site de dégradation de talus dans une zone résidentielle du sud de la Californie et compacté dans un conteneur en plexiglas à trois rapports de vide différents et trois inclinaisons différentes. Ces pentes ont été équipées de plusieurs tensiomètres miniatures et de dispositifs de mesure de déplacement à différentes profondeurs, puis soumises à deux intensités différentes de précipitations jusqu'à ce que toute la pente soit saturée. La variation de l'aspiration et l'avancement du front de mouillage ont été enregistrées à un intervalle régulier pour calculer la vitesse d'infiltration. De plus, une pente, munie de nombreux accéléromètres, a d'abord été secouée sur une table de tremblement avec diverses amplitudes et fréquences de mouvements sismiques puis soumise à un événement de pluie pour évaluer le changement de vitesse d'aspiration et d'infiltration après les secousses. Les résultats expérimentaux, vérifiés par des analyses numériques, ont été utilisés pour évaluer la relation entre l 'intensité des précipitations, le rapport des vides, l' inclinaison de la pente et la stabilité correspondante de la pente.

KEYWORDS: slope stability, compacted fill, unsaturated soil, suction, tensiometer, wetting front, seepage velocity, soil deformation.

1 INTRODUCTION

Development of expensive residential sub-divisions on or along slopes, especially near oceans and scenic view points is common in southern California. When building infrastructures on slopes, specifically on the embankments and compacted fills, it is important to evaluate the potential slope failure during rainfall and/or earthquake events. The construction quality control for highway embankments is more rigorous compared to construction on the compacted fills for new residential subdivisions. When rainwater infiltrates a slope, the stability of the slope decreases due to a loss of soil suction and an increase in soil density. Moreover, when the saturated slope is shaken by an earthquake, stability of the slope further decreases. In this study, slope near a residential building constructed at a developed subdivision in southern California was evaluated for possible slope instability issue due to an earthquake followed by rainfall events. The site is located in Mission Valejo, California and had a history of landslides due to intense rainfall few years following construction.

2 MATERIALS AND METHODS

Field investigations were conducted at the study area to obtain the cross-section of the slope, measure the in-situ void ratio of the soil and collect soil samples for physical modeling and laboratory experiments (Figures 1 to 3).

Laboratory tests were performed to evaluate the geotechnical properties of soil using pertinent ASTM standards. Few among the geotechnical properties that were measured in the laboratory include the specific gravity, grain size distribution, Atterberg limits, maximum dry density and optimum moisture content, hydraulic conductivity of soil, and soil-water characteristic curves.

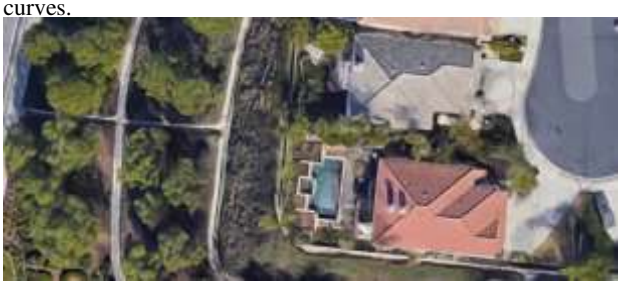

Figure 1. Bird's eye view of the soil sampling area.

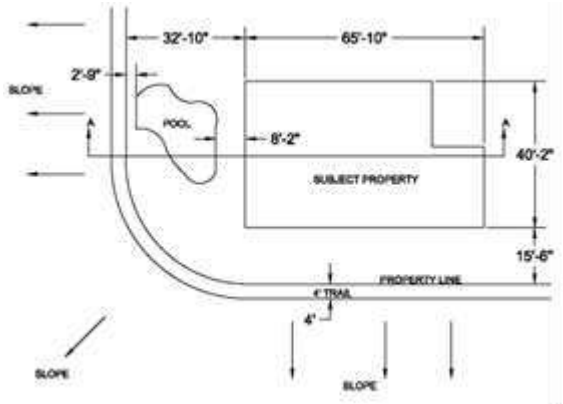

Figure 2. Plan view of the soil sampling area.

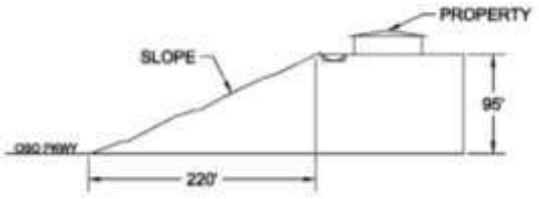

Figure 3. Cross-section of the soil sampling area.

Soil samples collected from the site were first passed through US sieve #4 and naturally dried. Then, the soil samples were compacted in a watertight Plexiglas container having dimension of 1.2 m x 1.2 m x 1.2 m at a lift thickness of 15 cm until the desired slopes and heights were achieved. The slopes were then instrumented with eight tensiometers distributed throughout the area (Figure 4) and eight straight vertical copper wires at different locations along the slope (Figure 5). The purpose of the tensiometer was to measure real time variation in soil suction with rainfall, while the copper wires were installed to measure the depth-wise deformation of the slope at the end of the experiment. The slopes were then, subjected to two different intensities of rainfall and the movement of the wetting front was measured until the slopes were completely saturated. Presented in Table 1 are the rainfall intensities, void ratios, and slope inclinations used to model different conditions for a parametric study.

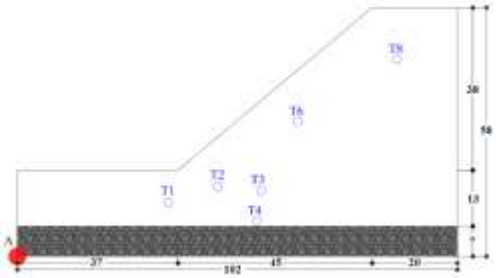

Figure 4. Location of (6 out of 8) tensiometers installed in the slope.

Figure 5. Picture showing the locations of tensiometers and vertical copper wires.

3 GEOTECHNICAL PROPERTIES OF SOIL

Geotechnical properties of the soils used in the experimental modeling are presented in Table 2. Values of drained friction angle and shear strength increase with suction (ϕ^b) were measured with controlled direct shear tests. Details of the laboratory testing procedures can be found in Caballero (2014) and Tran (2016).

4 RESULTS OF EXPERIMENTAL MODELING

Shown in Figure 6 is a typical record of the movement of the wetting front with time for model 2. Locations of the tensiometers are also presented in the figure. Also shown in the figure is the swelling of the slope after the completion of the experiment. Shown in Figure 7 is the suction recorded by the tensiometers. Three out of tensiometers malfunctioned in this model experiment. As can be observed in Figures 6 and 7, the time required for the wetting front to reach the tensiometer and vanish the suction matched well with the tensiometer recordings except in tensiometer 3. The wetting front data from all four sides were used later to calculate the seepage velocity. Similar figures for each model examined in this study are available in Tran (2016).

Table 1. Details of model experiments that were prepared and evaluated in this study.

Model #	*Slope inclination (degree)*	*Void Ratio*	*Rainfall Intensity (cm/h)*	*Acceleration (xg) & Frequency*
1	40	0.89	1.68	0
2	40	1.00	1.68	0
3	40	1.20	1.68	0
4	40	1.20	3.60	0
5	40	0.89	3.60	0
6	45	0.89	3.60	0
7	45	1.00	3.60	0
8	45	1.20	3.60	0
9	45	1.00	1.68	0
10	24	0.89	3.60	0
11	40	1.2	3.60	0.1-0.3;1-3 Hz

Table 2. Geotechnical properties of the soil used in this study.

Geotechnical Property	*Value*	*Geotechnical property*	*Value*
% of clay	20.0	% of silt	65.0
% of sand	15.0	Sp. gravity	2.69
Liquid limit	57	Plasticity index	30
$\gamma_{d,max}$ (kN/m^3)	17.3	W_{opt} (%)	15
K@ e=0.89 (x10^{-7}cm/s)	4	K@ e=1.2 (x10^{-7}cm/s)	9
ϕ' (deg)	25.7	ϕ^b (deg)	27.2

All of the experimental laboratory data were used to develop the relationship between seepage velocity, void ratio, slope gradient and intensity of rainfall. As can be seen in Figures 8 to 10, seepage velocity geometrically increases with an increase in the void ratio. Likewise, seepage velocity also increases with an increase in infiltration rate.

As the experimental study was prepared for small scale models and only for two different rainfall intensities, three different slope gradients and three different void ratios, the remaining parametric studies were performed using SEEP/W of GeoStudio 2016. As presented in Figure 11, the seepage velocity measured in the experiment and obtained from the numerical analysis after inputting appropriate parameters

matched well. Verifications of all models are available in Tran (2016).

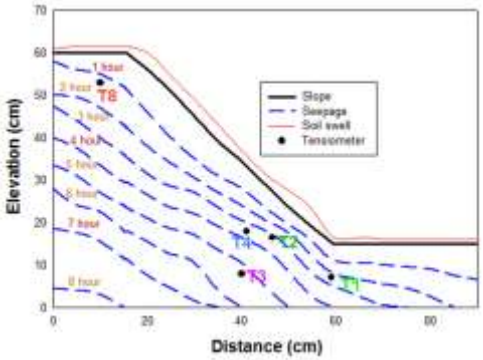

Figure 6. Movement of wetting front with time and amount of swelling of the slope at the end of the experiment.

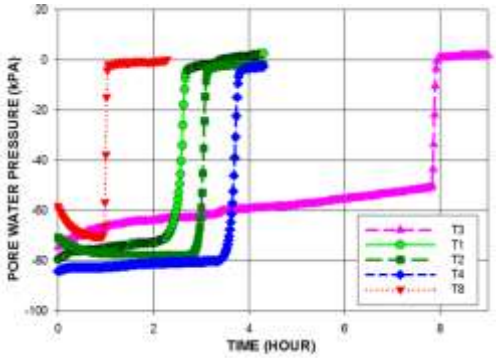

Figure 7. Variation of soil suction recorded by the tensiometers.

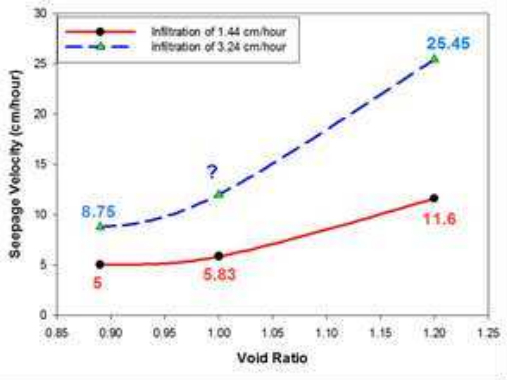

Figure 8. Relationship between seepage velocity, void ratio and infiltration rate (calculated based on the intensity of rainfall and runoff water).

The depth-wise deformation of copper wire at the completion of the experiments were plotted along the slope to obtain potential critical failure surface, as presented in Figure 12. The deformation data was later verified with the coupled seepage and deformation analyses performed using SEEP/W coupled with SIGMA/W of GeoStudio 2016, as presented in Figure 13. Similar results for the remaining models may be found in Tran (2016).

Model 11 was prepared on a shake table and was subjected to different magnitude and frequencies of seismic shaking followed by a rainfall intensity of 3.6 cm/h. The result of the study shows that the seepage velocity after the shaking event decreased by approximately 40%. This is mainly due to a reduction in void ratio of the slope as a result of the seismic loads. The deformation and seepage velocity data obtained from the laboratory experiments were used to verify the numerical results obtained by coupling the SEEP/W, SIGMA/W, SLOPE/W, and QUAKE/W of the GeoStudio 2016.

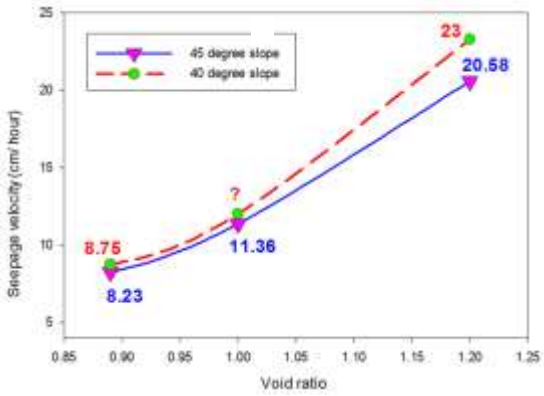

Figure 9. Relationship between seepage velocity, void ratio and slope.

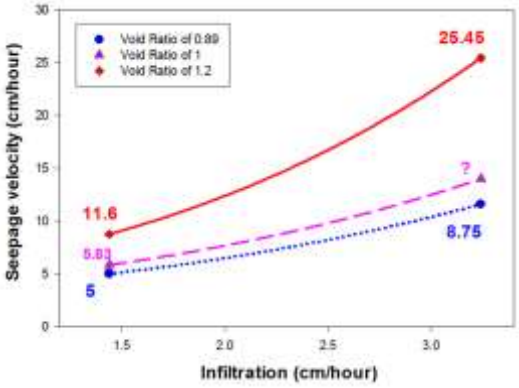

Figure 10. Relationship between seepage velocity, void ratio and infiltration rate.

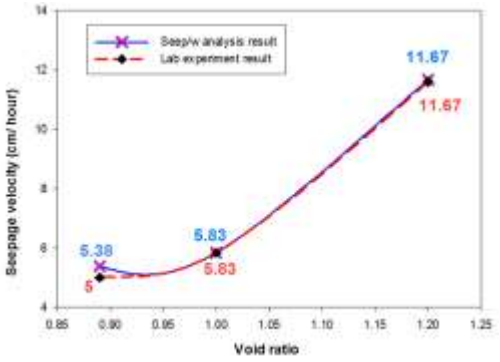

Figure 11. Verification of the relationship between seepage velocity and void ratio obtained from the numerical method using experimental

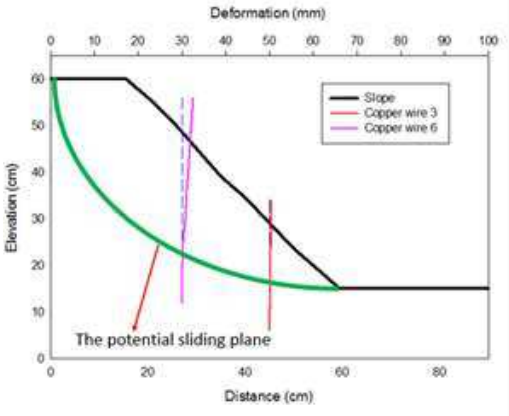

Figure 12. Potential failure plane obtained with the depth-wise deformation of copper-wire.

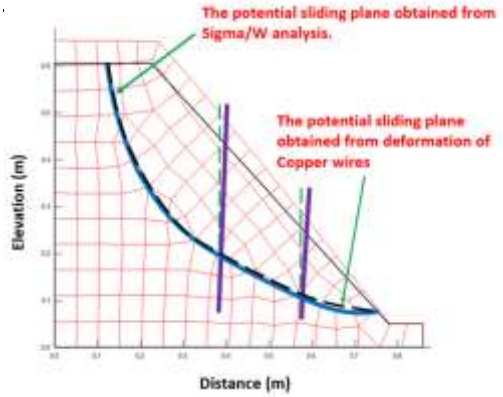

Figure 13. Verification of failure plane with numerical analysis.

5 NUMERICAL ANALYSIS OF THE STUDIED SLOPE

After verification of the numerical analysis results with experimental results, the slope presented in Figures 1-3 was analyzed with coupled seepage, deformation, and stability analyses using SEEP/W, SIGMA/W and SLOP/W of the GeoStudio 2016. The deformation analysis mesh is presented in Figure 14. The rainfall intensity of 3.6 cm/h was used for the analysis. For the numerical analysis, the field parameters tested in Model 10 were considered. For dynamic analysis, the seismic parameters mentioned in Model 11 were used.

Presented in Figure 15 is the change in factor of safety of the slope with duration of rainfall after the application of rainfall for static slope condition as well as for the factor of safety of slope subjected to an earthquake followed by a rainfall event. As can be observed in Figure 15, static factor of safety was lower than the post-earthquake factor of safety for the reasons mentioned earlier. If continuous rainfall for 14.2 hours were to occur, the factor of safety will drop to less than 1 to cause failure. However, if the same slope is subjected to earthquake events, densification of soil reduces seepage velocity and inceeases factor safety of the slope with duration of rainfall. The slope will require 24 hours of continuous rainfall at the intensity of 3.6 cm/h to cause failure on the same slope. The results presented in this study are very important as the slopes compacted at lower relative densities, i.e. higher void ratios, settle after seismic loading increasing the soil density. This will reduce the seepage velocity in the slope and increase the factor of safety of the slope.

6 CONCLUSION

Laboratory experiments were performed on soils collected from a housing development site in Southern California to quantify the effect of void ratio, slope gradient, and intensity of rainfall on the seepage velocity and slope deformation. Based on the results obtained from this study, the following conclusions can be made:

- Seepage velosity increases geometrically with an increase in void ratio and an increase in the intensity of rainfall as well as a reduction in the slope gradient.
- Change in seepage velocity after an earthquake event depends on the relative compaction of the soil. For slopes having low relative compaction, the soil densifies after seismic loading and seepage velocity decreases as compared to the soil prior to seismic loading.
- For the case study, a continuous rainfall for more than 14 hours with a constant rainfall intensity of 3.6 cm/h is required to drop the facor of safety below 1 and cause failure.

- The results presented in this study can be used for any type of soil slope and for any intensity of rainfall in order to perform a parametric study to evaluate the threshold rainfall intensity and duration to cause failure.

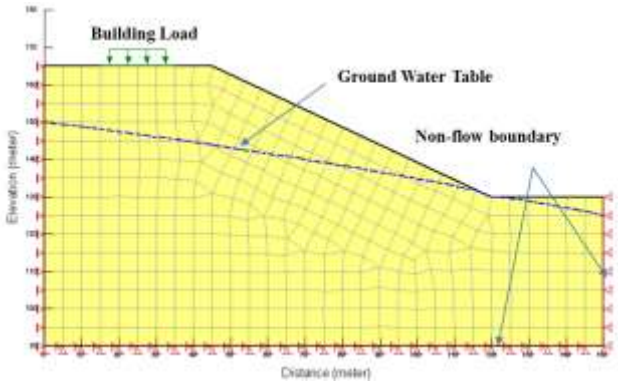

Figure 14. Deformation analysis mesh prepared for the case study slope presented in Figures 1-3.

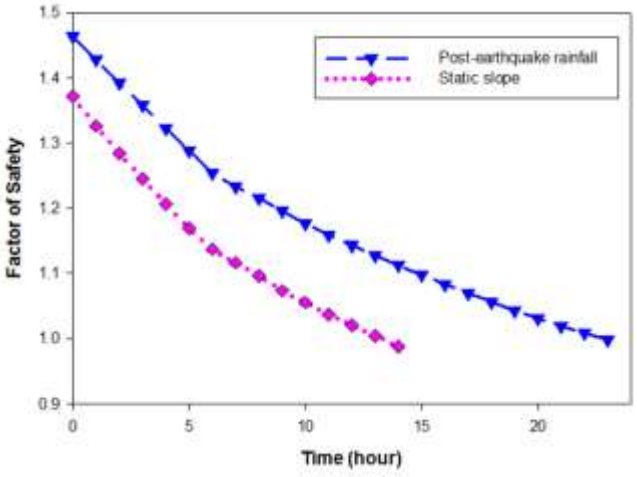

Figure 15. Factor of safety obtained from SLOPE/W (for static analysis) and QUAKE/W (for dynamic analysis) for the study slope.

4 REFERENCES

Caballero S. 2014. Experimental model of rainfall induced slope failures in compacted clays. *MSc Thesis submitted to the Civil and Environmental Engineering department, Californioa State University, Fullerton.*

Tran D. 2016. Effect of rainfall and seismic activities on compacted clay slopes having different void ratios and inclinations. *MSc Thesis submitted to the Civil and Environmental Engineering department, Californioa State University, Fullerton.*

Geo-Slope INTERNATIONAL. (2016). SLOPE/W 2016.

Geo-Slope INTERNATIONAL. (2016). SEEP/W 2016.

Geo-Slope INTERNATIONAL. (2016). SIGMA/W 2016.

Geo-Slope INTERNATIONAL. (2016). QUAKE/W 2016.